# THERMODYNAMIC SIMULATION OF THE ENDPOINT CHARACTERISTICS IN A CIGS DEPOSITION PROCESS

U. Zimmermann, J. Schöldström, M. Edoff, and L. Stolt
Ångström Solar Center, Uppsala University
Box 534, SE-751 21 Uppsala, Sweden

ABSTRACT: The purpose of this investigation was to model the thermodynamic behavior of a $Cu(In,Ga)Se_2$ sample during the growth process and especially during the conversion from copper-rich to copper-poor material in a two-step process. Starting from a very simple model of a directly heated substrate the model was refined until it qualitatively and quantitatively explained the features observed in the real experiment. The results can be used to determine more accurate criteria for the endpoint detection in a real-world evaporation system.
Keywords: $Cu(In,Ga)Se_2$ -1; Deposition -2; Simulation -3.

## 1 INTRODUCTION

The absorber layer in $Cu(In,Ga)Se_2$ (CIGS) based solar cells can be deposited directly from the vapor phase of the constituting elements. It is commonly known that the absorber layer has to be slightly copper deficient to result in effective solar cells, while the presence of a copper rich layer during growth favors the formation of larger, columnar grains. In order to overcome these contradicting premises several two- and three-stage processes have been reported in the past all of which have in common that the stoichiometry of the layer is changed during the ongoing growth, going back to the original Boeing recipe [1].

Following a modified version of the original Boeing recipe referred to as ***copper-rich-off*** (CURO) the deposition is performed in two steps: First a layer of copper-rich material ([Cu]/[In+Ga] > 1) is deposited onto the heated, molybdenum-coated glass substrate. After a certain period of time the copper source is turned off while a flux of indium and gallium is maintained in the presence of selenium vapor. In this final growth phase the CIGS layer is converted to the absorber-quality, slightly copper-poor material with a copper to combined indium plus gallium ratio of [Cu]/[In+Ga] ≈ 0.90.

It has been observed that different stages of the growth process and the different compositions of the CIGS material can be characterized by different thermal properties of the sample [3, 4]. This empirical knowledge has resulted in the development of an endpoint detection scheme to determine the final stage of the absorber growth based on significant changes in sample temperature at a constant heater power or changes in required heater power while keeping the sample temperature constant, respectively [5].

In order to gain a better understanding in the processes which lead to the observation of macroscopic temperature steps in the evaporation equipment during the transition from copper-rich to copper deficient CIGS we performed a series of computer simulations of the heat transfer under various conditions. The results of these simulations should help us to control the process conditions more accurately.

## 2 EXPERIMENTAL

The evaporation equipment used in our laboratory has been described in detail earlier [2]. Three modified Luxel Radak II sources are used to co-evaporate the metals while selenium is evaporated in excess from a quartz crucible. The CIGS film growth occurs on a radiatively heated molybdenum coated soda-lime glass substrate.

Fig. 1 shows the measured substrate temperature at six locations on a 10×10 $cm^2$ glass substrate during a CIGS deposition following the CURO recipe. The substrate temperature in our evaporation setup is monitored by K-type thermocouples. These thermocouples have the thermojunction hermetically sealed inside a 0.5 mm diameter stainless steel tube which is mechanically pressed against the backside of the substrate. This experiment was performed at constant heater power rather than constant substrate temperature, as described in [5].

At the time before the deposition process is started the glass substrate is approaching thermal equilibrium with the surrounding heater box. The sharp drop in temperature at $t = 0$ min correlates to the start of the growth of copper-rich CIGS material. The following rise in temperature at about $t = 12$ min correlates to the transformation of the CIGS layer into a copper-deficient composition after the copper source has been turned off while the deposition continued under a flux of indium and gallium in the presence of selenium vapor.

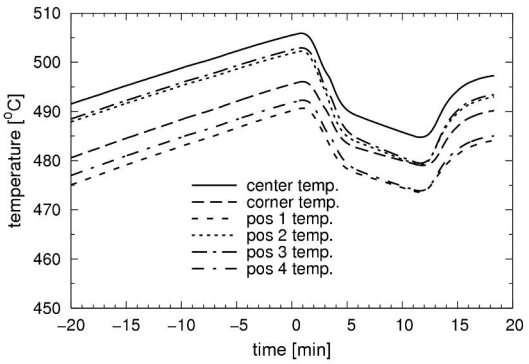


**Figure 1:** Measured substrate temperatures at six different locations on a 10×10 $cm^2$ sample during a CIGS deposition process. Growth is started at time $t = 0$ min.

During this last stage of the deposition excess copper from the already deposited layer is consumed at the growth surface and the originally copper-rich CIGS layer is converted into increasingly copper-poor CIGS material. The degree of conversion has previously been

evaluated by extracting samples at certain points along the process run and measuring the composition by means of X-ray fluorescence (XRF) and energy dispersive spectroscopy (EDS).

The total emissivity ε at room temperature has been determined optically for CIGS samples with known lateral gradients in copper concentration extending from copper-poor to copper-rich composition. A range between $\varepsilon = 0.10$ for the emissivity of copper-poor and $\varepsilon = 0.45$ for copper-rich material was found.

## 3 THEORETICAL MODEL AND SIMULATION

In order to reveal the thermodynamic processes behind the endpoint detection scheme finite element simulations have been carried out. These simulations require an accurate model of the physical system to produce meaningful results.

Our model takes into account the radiative heating of a stainless steel heater block from a constant temperature heat source - the infrared lamps in our real-world setup. This heater block itself is in radiative thermal equilibrium with the backside of the glass substrate.

The sample was modeled as a 1 mm thick glass plate where the emissivity of the backside was assumed to be determined by the substrate glass itself while the emissivity of the frontside was varied during the simulation, according to the experimentally observed change in the emissivity of the deposited layers. This change in emissivity was provided by a time series with smooth transitions between the assumed equilibrium emissivities, as depicted in Fig. 2. Values for the thermal properties of the common materials were taken from the literature [7].

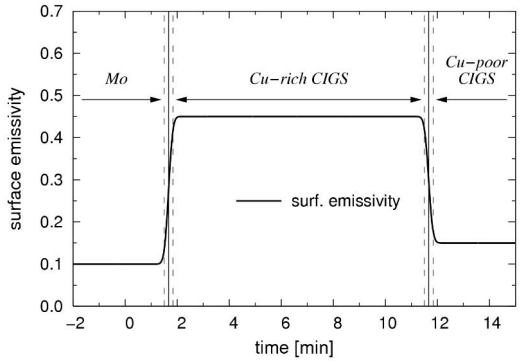


**Figure 2:** Modeled change in emissivity during CIGS deposition from the pure molybdenum backside contact via the copper rich phase into the copper deficient phase. Growth is started at time $t = 0$ min.

The sample geometry was constructed as a two-dimensional heat transfer model in the finite element solver FEMLAB [8]. The simulations were conducted on mesh grids with about 150-200 node points. The models were refined to subsequently contain more of the real-world parameters, such as the temperature dependent emissivities and specific heats of the used materials.

In the final model the sample temperature during simulation is monitored by means of small probes in contact with the back surface of the sample instead of reading the temperature in the surface nodes directly. This corresponds to the thermocouple probes used in out real-world setup and led to an improved correlation between the experimental results and the simulation.

The basic differential equations which have to be solved in the two dimensional heat transfer model are the heat transfer in the bulk of the materials and the heat transfer at the surface of the structures (or domains). These are readily implemented in the numerical solver for partial differential equations (PDE) of the FEMLAB package.

## 4 RESULTS AND DISCUSSION

After the first simulations it became clear that the measured difference in emissivity on samples with differences in copper contents would be sufficient to explain the experimentally observed evolution in substrate temperature during the CIGS deposition. Assuming a directly heated backside of the substrate even overestimated the temperature steps by a factor of 2 – 10. Also in this case the simulations predicted a constant substrate temperature during a large fraction of the deposition of the copper-rich CIGS layer, which did not correspond to the experimental results.

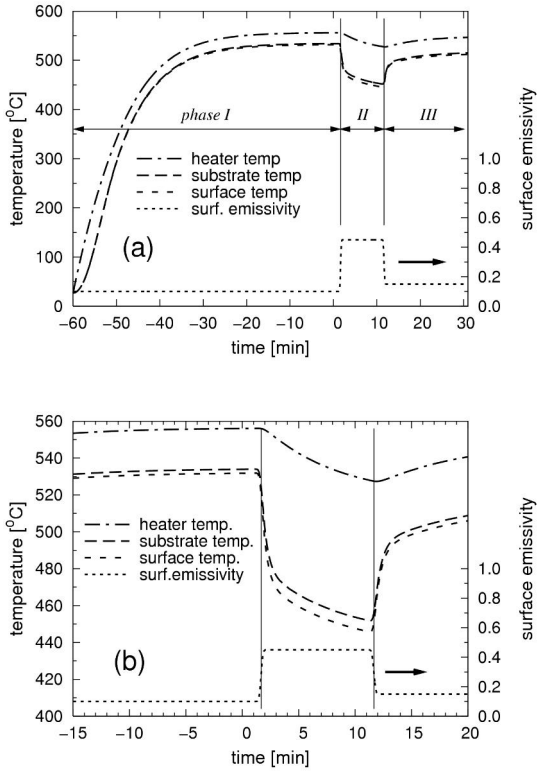


**Figure 3:** Simulated temperature progressions during CIGS deposition. During phase I the system approaches thermal equilibrium before the deposition is started. Copper-rich CIGS with a high emissivity is deposited in phase II and converted into copper deficient CIGS at the beginning of phase III. An enlarged view of phase II is shown in (b).

In the final model the direct heating of the sample was replaced and the thermal mass of the heater block was introduced, as described above. The simulation results now accurately predict the continuous drop of the

substrate temperature during the deposition of Cu-rich CIGS in phase II as seen in Fig. 3, compared to the experimental curves in Fig. 1.

According to our simulations this drop in temperature can be attributed to the loss of thermal energy from the massive heater block by the increased emission of the sample surface, due to the higher emissivity of copper-rich CIGS as compared to the originally molybdenum-coated glass substrate. The sample temperature itself quickly follows the abrupt changes in emissivity which corresponds well to our experimental results. Further simulations were performed on this model where the slope of the change in emissivity was changed for the transition between Cu-rich and Cu deficient CIGS, which in the scope of the accuracy of our model only had minor influence on the observed changes in substrate temperature.

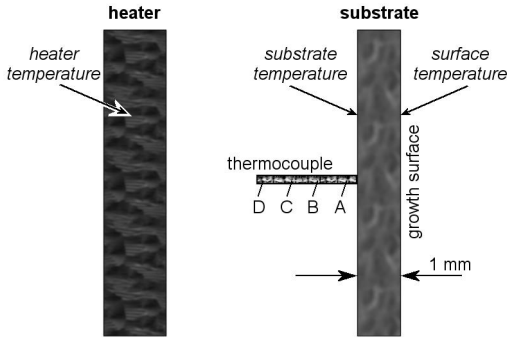


**Figure 4:** Schematic diagram over the model showing the relative location of the substrate and the heater. A thermocouple is modeled as a massive rod in thermal contact with the backside of the substrate. Points A to D mark assumed locations of the thermojunction inside the rod (drawing not to scale).

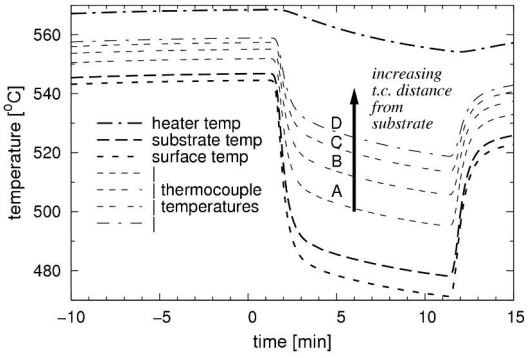


**Figure 5:** Simulated temperature at the assumed junction location inside the thermocouple rod (points A to D). Since the rod itself is also radiatively heated from the heater, the observed temperature increases with the distance from the substrate.

Since the substrate temperature in our evaporation setup is monitored by means of thermocouples with a thermojunction at a certain distance from the substrate we can expect a thermal gradient between the real substrate interface and the sensing junction. This was modeled assuming a stainless steel rod in perfect thermal contact to the backside of the substrate, as depicted in Fig. 4. As shown in Fig. 5 the observed temperature along this rod increases with increasing distance from the substrate because of the proximity of the thermocouple to the heater. At the same time the magnitude of the observed temperature steps decreases with increasing distance from the substrate. This could explain the still larger temperature steps predicted by the simulations as compared to the experimental data (see Fig. 1).

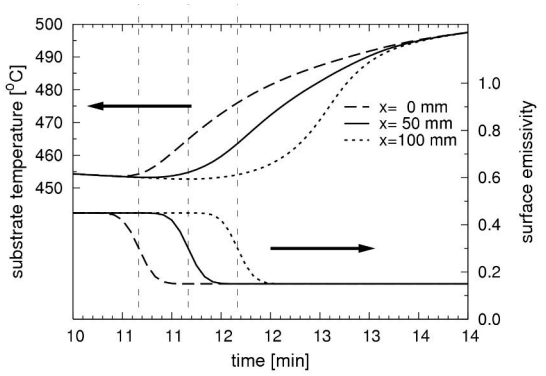


**Figure 6:** Simulation result showing the lateral propagation of the observed temperature step as a result of a laterally delayed conversion from the copper-rich to the copper deficient composition. The transition starts at x = 0 mm and proceeds towards x = 100 mm as modeled by the local emissivity. The temperature step observed at the backside of the substrate follows immediately.

Due to the geometry of our real-world evaporation system and the arrangement of the evaporation sources our samples always show a lateral gradient in copper concentration. Assuming the simple growth model outlined above this would result in a temporal delay for the transition between Cu-rich (phase II) and Cu deficient (phase III) CIGS growth at different lateral locations on the sample. The effect on this delay on the substrate temperature observed at different locations on the backside of the sample can be seen in Fig. 6. Here the transition time was delayed by 1 min between two edges of the substrate 100 mm apart. The temperature step observed in the simulations at selected locations on the backside follows the proceeding change of emissivity on the frontside almost immediately, which is a reasonable finding considered the small thickness (1 mm) of the glass substrate compared to the lateral dimensions (100 mm) of the sample.

## 5 CONCLUSIONS

We have shown that the observed temperature progressions during the CIGS deposition according to the two-step CURO process can be fully explained by the change in emissivity of the sample surface during the different phases of the growth process. First the emissivity changes from the comparatively low value of pure molybdenum to the observed higher value of copper-rich Cu(In,Ga)$Se_2$ after the very few layers of this material have been deposited. This change in emissivity leads to an increase in heat transfer from the sample surface which also affects the total heat loss of the substrate heater assembly.

When the system is heated with a constant power this

heat loss can be monitored as a sudden drop in sample temperature followed by a more slightly decrease of temperature of the whole heater assembly towards a new thermal equilibrium at a lower average temperature. When the stoichiometry of the deposited CIGS layer reaches a copper-deficient state after the copper source has been turned off, the emissivity of the deposited layer drops significantly and gives rise to an increase in substrate temperature. This second step can be used to indirectly monitor the sample composition during growth and stop the growth process when the desired stoichiometry has been reached.

Using accurate calibration of the simulation parameters it should be possible to use the simulation results directly to determine suitable endpoint criteria for a desired CIGS composition in the described CURO two-stage process. The accuracy of the simulation could certainly be further increased by using a full-scale three dimensional model of the evaporation equipment, however, it has to be debated in which way this would lead to a deeper understanding of the involved thermodynamic processes.

## 6 ACKNOWLEDGMENTS

This work was carried out within the framework of the Ångström Solar Center and financially supported by the Foundation for Strategic Environmental Research (MISTRA) and the Swedish National Energy Agency.

## 7 REFERENCES

[1] R. A. Mickelsen and W. S. Chen, Proc. 15th IEEE Photovoltaic Specialists Conference (1981) 800-804.
[2] J. Kessler, C. Chityuttakan, J. Lu, J. Schöldström, and L.~Stolt, Progr. Photovoltaics: Res. Appl. 11 (2003) 319-331.
[3] N. Kohara, T. Negami, M. Nishitani, and T. Wada, Jpn. J. Appl. Phys., Part 2 (Letters) 34 (1995) L1141-1144.
[4] M. Nishitani, T. Negami, and T. Wada, Thin Solid Films 258 (1995) 313-316.
[5] J. Kessler, J. Schöldström, and L. Stolt, Proc. 28th IEEE Photovoltaic Specialists Conference (2000) 509-512.
[6] J. Kessler, J. Wennerberg, M. Bodegard, and L. Stolt, Sol. Energy Mat. Sol. Cells 75 (2003) 35-46.
[7] Lide, D. R. (editor), CRC Handbook of Chemistry and Physics, CRC Press (2003), ISBN 0849304849.
[8] FEMLAB Reference Manual, Comsol AB, Stockholm (2000).